

Melt layer damage simulation of first wall beryllium armour under heat load caused by ITER transient events

B. Bazylev¹, G. Janeschitz², I. Landman¹, S. Pestchanyi¹, A. Loarte³

¹Forschungszentrum Karlsruhe, IHM, P.O. Box 3640, 76021 Karlsruhe, Germany

²Forschungszentrum Karlsruhe, Fusion, P.O. Box 3640, 76021 Karlsruhe, Germany

³EFDA Close Support Unit Garching, Boltmannstr.2, D-85748 Garching bei München, Germany

Introduction

So far, most of the modeling effort on damage to plasma facing components (PFC) under transient loads in ITER was concentrated upon the divertor target [1-6]. Namely, a significant effort has been recently dedicated to study and model the damage to the divertor W and CFC armour for the disruptions and Type I ELM loads [1-6]. It seems that a similar study for the main chamber wall Be-clad and Be-coated divertor armor plasma facing component (PFC) in ITER is also necessary, because significant heat loads during transient events are expected at the main chamber wall [7]. The expected thermal fluxes Q caused by the dumped plasma on the ITER PFCs during ITER transients are: I) *Divertor target*: Type I ELM: $Q = 0.5\text{--}4 \text{ MJ/m}^2$ on the timescale $\tau = 0.3\text{--}0.6 \text{ ms}$; Disruption thermal quench: $Q = 2\text{--}13 \text{ MJ/m}^2$, $\tau = 1\text{--}3 \text{ ms}$. II). *First wall (FW)*: Type I ELM: $Q = 0.5\text{--}2 \text{ MJ/m}^2$, $\tau = 0.3\text{--}0.6 \text{ ms}$. The thermal quench: $Q = 0.5\text{--}5 \text{ MJ/m}^2$, $\tau = 1\text{--}3 \text{ ms}$. The pressure and the energy distributions of the dumped plasma over the FW are not exactly known. The mitigated disruptions stimulated by massive noble gas injection into ITER vessel generate radiative loads at the FW $Q = 0.1\text{--}2 \text{ MJ/m}^2$ and $\tau = 0.2\text{--}1.0 \text{ ms}$. The intense radiative heat loads at the first wall surface may also be caused by the tungsten or carbon vapor that has expanded into SOL from the divertor region after the ELMs and the disruptions.

The beryllium PFC components will be located at the main chamber wall of ITER (Be-clad blanket modules in macrobrush design with brush size of 8-10 cm). The aim of this work is to provide reliable estimations of the damage to the Be-clad blanket modules under the mentioned Type I ELM and the disruption thermal quench loads.

The numerical simulations completed for the tungsten armors demonstrated: In the ITER even for moderate and weak ELMs, where a weak shielding layer does not protect the armour surface from the dumped plasma, the main mechanisms of metallic armour damage remain the

surface melting and melt motion erosions caused by the direct action of dumped plasma on the target surface. The magnitude of total erosion depends on target design and such parameters of the impacting plasma as the inclination angle and the dynamic plasma pressure ρv^2 , with ρ the plasma density and v the plasma velocity. The simulations demonstrated also that armour macrobrush structure can prevent violent melt motion for the Type I ELMs and moderate disruptions, which significantly decreases the final magnitude of melt erosion.

The results of numerical simulations (using the code MEMOS) of the erosion due to evaporation and estimation of the melt layer thickness under expected ITER ELM-like heat loads $Q = 0.2$ to 2 MJ/m^2 and the pulse durations $\tau = 0.2$ to 0.6 ms (both radiative and plasma with account for vapor shielding) are presented. The melt motion damage of Be macrobrush armour caused by the tangential friction force is analyzed for different sizes of Be-brushes: 1, 2, and 4 cm and compared with the bulk Be target. Numerical simulations have demonstrated that for Be-brushes of 1 and 2 cm the melt motion damage is much less than it is observed in the bulk Be armour. The damage of FW under radiative heat arising during mitigated disruptions is estimated. The numerical simulations of such type of disruptions are carried out using the code FOREV for the release of 90, 130, 170 and 390 MJ of the plasma energy during 3 ms. The radiative heat loads at the FW obtained in FOREV calculations are transferred into the code MEMOS as input data and further MEMOS simulations are carried out.

Numerical simulations of Be armour erosion.

Bulk Be-armor erosion: melting and evaporation thresholds. The final Be armour damage

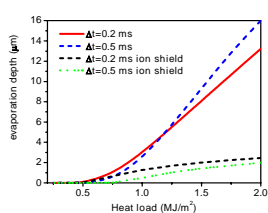


Fig.1. Dependence of evaporation depth on the heat load.

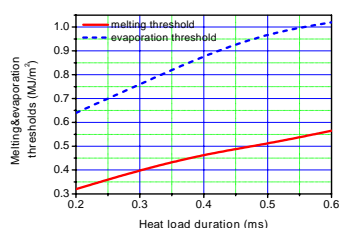


Fig.2. Dependence of melting and evaporation thresholds on heat load duration.

significantly depends on heat load source: either dumped plasma or radiation heats the armour surface. In case of plasma impact ionized vapor shield protects the surface from the most intense impact of hot plasma.

That leads to significant decreasing the erosion due to evaporation in comparison with the radiation action at the armour surface. In the last case shielding is negligible. The dependences of evaporation depths on the energy heat load for $\tau = 0.2 \text{ ms}$ and $\tau = 0.5 \text{ ms}$ calculated by the code MEMOS are presented in Fig. 1. With the vapor shielding, maximum evaporated material thickness slightly exceed $2 \text{ }\mu\text{m}$ whereas the

radiation heat load leads to monotonic growth of evaporated material thickness. The calculated dependences of melting and evaporation thresholds on the heat load duration for the Be armour is shown in Fig. 2.

Be macrobrush armour erosion caused by the melt motion. Numerical simulations of Be clad damage caused by the plasma stream action are carried out for the Be bulk and macrobrush designed armour in the following assumptions. The sizes of the macrobrush elements are the following: the diameter of brushes $D = 1$ cm, 2cm, and 4 cm and 8 cm, the depth of the gaps between the brushes $h = 1$ cm, the width of the gaps is equal to 1 mm. The macrobrush edges are assumed as convex corners rounded with a radius R of 1.5 mm. It is assumed that the Be target is heated with the energy deposition of the Gaussian spatial profile with the half-width $H_w=10$ cm and the plasma beam width 15 cm ($x_0 = 15$ cm). To investigate influence of the tangential friction force (as mostly important driving force [3-6]) on the Be-brush target damage several scenarios with the peak energy deposition $Q_0 = 1 \text{ MJ/m}^2$ and the tangential friction force (applied in the opposite direction to the x axis), which are expected in ITER $p_{\parallel} = 0., 0.01, 0.02$ bar, were calculated. For all scenarios the reference heat load durations $\tau = 0.5$ ms with the rectangular pulse shape are assumed.

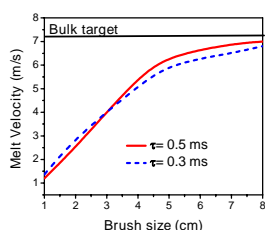


Fig. 3. V_{\max} vs. brush sizes. $Q = 1 \text{ MJ/m}^2$, $p_{\parallel}=0.02$ bar. .

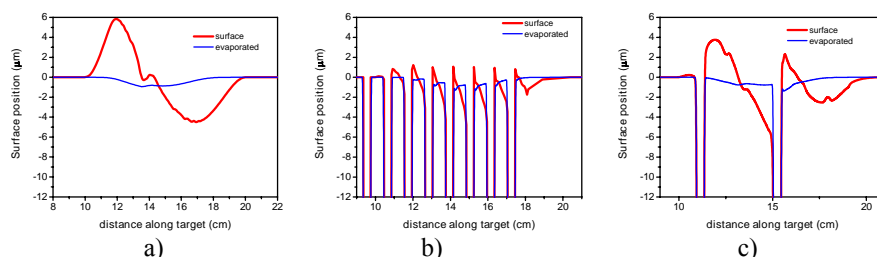


Fig. 4. Final erosion profile of Be armour. $Q = 1 \text{ MJ/m}^2$, $\tau = 0.5$ ms, $p_{\parallel} = 0.02$ bar, a) bulk target, b) brush size $D= 1$ cm, c) brush size $D= 4$ cm

The numerical simulations demonstrated that maximum depths of melt pool both for the bulk and macrobrush targets are practically the same being about $40 \mu\text{m}$ for. The tangential friction force generates violent melt motion with the velocities (V_{\max}) exceeding 7 m/s at the bulk target, about 1.2 m/s at the Be-brush target with $D=1$ cm and 5.5 m/s for $D=4$ cm and about 7 m/s for $D=8$ cm (Fig. 3). In the case of bulk Be target the height of the mountain at the left side of the heated region is $6 \mu\text{m}$ and the depth of the crater from the opposite side is about $5 \mu\text{m}$ (Fig.4a). For the Be-brush targets violent melt motion shifts the melt layer of each brush element from the frontal edge to the back-edge (Fig. 4b and 4c, in which erosion profile for the Be-brush target

with $D = 1$ cm and 4 cm are shown). In all these figures the erosion due to material evaporation is also indicated. The damage to the macrobrush targets with the sizes $D \leq 2$ cm is significantly less in comparison with that of bulk Be armour. The maximum magnitude of mountains at the back-edge at $D=1$ and $D=2$ cm is about $2 \mu\text{m}$, whereas for the Be-brush target with $D = 4$ cm the maximum magnitude of mountains at the back-edge is comparable with that of bulk Be armour.

Be first wall damage under radiative heat load during mitigated disruptions. The scenarios of mitigated disruptions with the release of 90, 130, 170 and 390 MJ of the plasma energy during 3 ms were simulated by the code FOREV to obtain the radiation fluxes at the FW. These fluxes are used as input data in the MEMOS simulations. Numerical simulations demonstrated that Upper and Outer walls are the mostly irradiated regions. The disruption scenarios, in which carbon

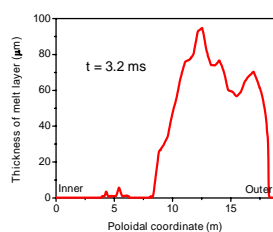


Fig. 5. Distribution of melt pool depth along poloidal coordinate

plasma expands from the divertor region with negligible penetration into the pedestal (90, 130, 170 MJ), are not so dangerous for the FW. The maximum of the surface temperature does not reach the melting temperature remaining below 1100K. In case of the higher energy release (390 MJ), in which the carbon plasma penetrates in the pedestal in considerable quantities, radiation fluxes at the FW significantly increase practically along the entire FW. That leads to

significant increase of the surface temperature above to 2000K and melting Be armour along approximately 10 m after 1.5 ms. The depth of the melt pool reaches $100 \mu\text{m}$ at the Upper wall that can be seen in Fig. 5. So high surface temperature of the Be armour leads also to essential evaporation of Be in average of about $0.5 \mu\text{m}$ on distance about 5 m along the Upper wall. Maximum evaporation depth reaches $1.7 \mu\text{m}$.

This work, supported by the European Communities under the contract of Association between EURATOM and Forschungszentrum Karlsruhe, was carried out within the framework of the European Fusion Development Agreement. The views and opinions expressed herein do not necessarily reflect those of the European Commission

References

- [1] B. Bazylev, H.Wuerz, J. Nucl. Mater. 307-311 (2002) 69-73. [2] B. Bazylev et al., Europhysics Conference Abstracts, Vol. 27A, P-2.44. [3] B. Bazylev et al J. Nucl. Mater. 337-339 (2005) 766-770. [4] B.N. Bazylev et al Fusion Eng. Design. 75-79 (2005) 407-411. [5] B.N. Bazylev et al Physica Scripta. T128 (2007) 229-233. [6] B.N. Bazylev et al. J. Nucl. Mater. 363-365 (2007) 1011-1015. [7] A. Loarte et al, Proceedings of the 21st IAEA Conference Chengdu, 16-21 October 2006. ISBN 92-0100907-0/ ISSN 0074-1884.